2.4. STRUCTURAL TOXICITY / 2.4.2. HYPERTROPHY

In Stem Cell-Derived Models in Toxicology Book

Janos Kriston-Vizi[1], Sian E. Harding[2], Gábor Földes[2,3]

[1]MRC Laboratory for Molecular Cell Biology, University College London, London, United Kingdom
[2] National Heart and Lung Institute, Imperial College London, London, United Kingdom
[3] Heart and Vascular Center, Semmelweis University, Budapest, Hungary

Running head: hypertrophy models of hPSC-CM

Number of words:
Number of figures: 5

Correspondence:
Gabor Foldes, MD PhD
National Heart and Lung Institute
Imperial College London
Imperial Centre for Experimental and Translational Medicine
Hammersmith Campus
Du Cane Road
London W12 0NN
United Kingdom
Email: g.foldes@imperial.ac.uk

and

Janos Kriston-Vizi, PhD
Email: j.kriston@ucl.ac.uk

1. Abstract
Human pluripotent stem cells (hPSC) are investigated as a source of authentic human cardiac cells for drug discovery and toxicological tests. Cell-based assays performed using an automated fluorescence imaging platform and high content analysis are valuable in characterizing hypertrophic states that may be induced in hPSC-derived cardiomyocytes upon exposure to cardiotoxic compounds. In high-purity populations of hPSC-derived cardiomyocytes loaded with cell tracer probes and other cell markers, detailed hypertrophic profiles can be assessed based on information captured at cellular and subcellular levels.

Key Words: human pluripotent stem cells, cardiomyocyte, hypertrophy, automated high content imaging

2. Introduction. Cardiac hypertrophy is the abnormal enlargement of the heart muscle, resulting from a thickening of cardiomyocytes and changes in other heart muscle components, such as extracellular matrix, and can lead to heart failure. Physiological hypertrophy occurring in pregnancy and athletes is not detrimental and results in normal or enhanced heart function. Causes can also be pathological, as a result of pressure overload in response to hypertension or valvular disease.

2.1. Human pluripotent stem cell-derived cardiomyocytes (hPSC-CM). Human PSC are being investigated as a new source of cells for cardiac disease modelling. Predominant manifestations of cardiac pathologies investigated in engineered hPSC-CM are short-term, including depressed cell contraction, electrophysiological changes and arrhythmia, or longer-term, such as abnormal morphology, hypertrophy and increased susceptibility to cell death. While the acute characteristics show close similarities to those observed in adult cardiomyocytes, a marked difference in viability is seen in the long term survival (months) of hPSC-CM cultures compared to ex vivo adult cell cultures (~two days). This of course is one of the main attractions of hPSC-CM as a model system. Pharmaceutical companies are showing growing interest in using these cells for drug development and toxicology, hoping that these human cell-based platforms will increase predictive capabilities and decrease drug development costs.

A number of human induced pluripotent stem cell-derived cardiomyocyte (hiPSC-CM) models for genetic diseases have a hypertrophic phenotype, including the LEOPARD syndrome and hypertrophic cardiomyopathy (HCM) (Table 1). Human iPSC-CM of LEOPARD syndrome display increased cell size along with increased expression of nuclear factor of acti-

vated T-cells (NFAT) (Carvajal-Vergara et al. 2010). Patient-derived HCM hiPSC-CM exhibit increased basal cell size compared to controls (Tanaka et al. 2014; Lan et al. 2013). On the other hand, it still remains to be determined whether HCM patient-derived cardiomyocytes or control cells treated with hypertrophic stimuli are the best model to use for the study of hypertrophy. The majority of these disease models originate from patient-derived hiPSC, but the trisomy 21 model described by Bosman and co-workers utilises patient human embryonic stem cell-derived cardiomyocytes (hESC-CMs) (Bosman et al. 2015). In this study trisomic cells showed an increased expression of HCM genes in comparison to those in euploid control (Bosman et al. 2015). A greater understanding of hypertrophic signalling in hPSC-CM is required to ensure conclusions drawn from these models are physiologically relevant. In this chapter we describe scalable high content microscopy-based methods for the detection of cell growth and hypertrophy in hPSC-CM (using the assay measures such as cell area, volume, sarcomere organization, and atrial natriuretic factor (ANF) subcellular distribution) that can serve for personalised in vitro cardiomyocyte screens (Figure 1 and Table 2).

2.2 Intracellular signalling in hPSC-CM hypertrophy

We have reported an increase in cell size in hESC-CM in response to phenylephrine (PE) (Foldes et al. 2011), attributed to activation of p38 MAPK signalling pathways. It was found that a combination of small molecule inhibitors such as those targeting the STAT3 pathway can partially restore the PE response in hiPSC-CM. However, using pharmacological approaches, the hypertrophic response in hPSC-CM remains controversial. In contrast to hESC-CM, our results showed that hiPSC-CM are unresponsive to alpha-adrenergic stimuli, with cell size and ANF expression remaining unchanged (Foldes et al. 2014). In other studies, mild increases in hiPSC-CM size (10% or less) have been seen with alpha-adrenergic PE, and up to 25% with endothelin-1 (Tanaka et al. 2014). Data are also conflicting for the presence of cardiomyocyte hypertrophy in response to β-adrenergic stimulation. We found no increase in hiPSC-CM size (Foldes et al. 2014), whereas Zhi and colleagues found the opposite in HCM cells (Zhi et al. 2012). In that model, β-adrenergic stimulation exacerbated cellular hypertrophy as well as abnormal calcium handling and arrhythmia (Lan et al. 2013). Enhanced myofibrillar disarray and NFAT nuclear translocation were also reported (Zhi et al. 2012). It has been shown that serum-containing media causes hypertrophy in hESC-CM and hiPSC-CM, which may explain the lack of further cellular growth in response to hypertrophic stimuli in some studies (Dambrot et al. 2014).

We postulate that the difference between hESC-CM and hiPSC-CM is caused by an imbalance in anti-hypertrophic signalling pathways. The predominant α-adrenergic receptors (AR) in the myocardium are α_1-ARs (Bruckner et al. 1985), and stimulation with catecholamines induces pathological cardiac hypertrophy (Zhong and Minneman 1999; Rokosh et al. 1996). We found that the expression of α-ARs in hPSC-CMs shows an early and transient up-regulation during differentiation followed by a rapid down-regulation of α_{1A}-AR mRNA levels both in hiPSC-CM and hESC-CM. Conversely α_{1B}-AR was found to be increased in an apparently compensatory manner (Foldes et al. 2014). The analysis of signalling pathways identified an EGFR/Src/GSK3β/STAT3 network modulated by α_{1B}-AR that could drive the hypertrophic process.

Endothelin-A receptor (ET_A) is expressed in the cardiovascular system and has a number of roles including vasoconstriction, tachycardia, positive inotropy and hypertrophy (Concas et al. 1989; Bupha-Intr et al. 2012; Drawnel et al. 2013). We found that ET_A as well as angiotensin II (Ang II) and cyclic stretch can increase cell size in hESC-CM with corresponding increases in ANF expression (Foldes et al. 2014; Foldes et al. 2011). In hPSC-CM, ET_A also induces expression of hypertrophic genes such as BNP and ANF (Foldes et al. 2014). ET_A and Ang II did not result in significant increases in cell size and correspondingly increased ANF and BNP expression was only seen in response to ET_A activation. Hypertrophic modelling in commercially available hiPSC-CM assays relies therefore on detection of BNP expression in response to ET_A (Shamir and Ewald 2014).

2.3 3D high-content screening and 3D high-content analysis

Image-based 3D high-content screening is still in its infancy, even though a large body of literature has presented a rich set of 3D cell culture techniques in the past decades (Pampaloni et al. 2007; Ansari et al. 2013; Shamir and Ewald 2014; Debnath and Brugge 2005). Cell-based 3D high-content screening can be approached at tumour spheroid (Vinci et al. 2012; Kunz-Schughart et al. 2004) or single cell level (Foldes et al. 2014). Assessment of complex structural changes in cardiomyocyte hypertrophy, such as rearrangements of sarcomere structure and dynamic translocation of natriuretic peptides or transcription factors, requires 3D imaging. 3D high-content image acquisition requires a plate reader equipped with a high resolution microscope capable of optical sectioning (Ketteler and Kriston-Vizi 2016). We used an Opera LX spinning disk confocal plate reader (PerkinElmer) for 3D high-content image acquisition. The specifications of computer hardware for 3D high-content analysis (HCA) are similar to the 2D HCA. General HCA hardware considerations (Copeland and Shamu

2016) are applicable, however the extra spatial dimension requires the additional memory for image analysis and hard drive space for data storage that server-grade workstations can provide. For 3D HCA, third party, standalone software is currently preferred over the dedicated software solutions typically shipped with HCA imaging platforms (Ketteler and Kriston-Vizi 2016). Although the dedicated analysis solutions tend to be designed for the biologist with user friendly interfaces, they are typically intended to analyse common 2D assays, and are insufficient for analysis of 3D assays (Ghosh et al. 2007). We use ImageJ (Abramoff et al. 2016) for image analysis, and R (R Core Development Team 2016) for statistical data processing.

3. Materials

3.1. Human pluripotent stem cell-derived cardiomyocytes

1. Extracellular matrix Matrigel-coated plates as substrates for feeder-independent human ESC or hiPSC cultures.
2. Pre-defined stem cell qualified medium such as mTESR1 for culturing undifferentiated stem cells.
3. Serum-free basal medium for hypertrophy experiments: a. DMEM:M199 medium, in 3:1 ratio. Add 1 ml penicillin/streptomycin, 0.2 g bovine serum albumin (0.2% wt/vol), 0.00176 g ascorbic acid, 0.066 g creatine, 0.0626 g taurine, 0.03224 g carnitine to 100 ml DMEM/M199 medium. Dilute insulin 1:10 (final concentration 10 mg/ml) and then add 8.2 µl of this to 50 ml DMEM/M199 on the day of experiments. Alternatively, RPMI basal medium supplemented with B27 can be used for screening experiments.
4. For dissociation of cultures into single cardiomyocytes, remove media from cells and add TrypLE (0.5 or 1ml, Gibco) at room temperature (RT), and incubate for 8 min at 37 oC. Triturate cells 4 times and transfer to a 15ml tube. Spin 4 min at 240g. Remove media after spin. Add RPMI-B27 (with insulin) and triturate gently. Plate cells at the density desired ($5x10^5$ for 24-well plate and 750K for 12-well plate) and RPMI-B27 (with insulin). It can take 2-3 days to see beating cells.

3.2. Hypertrophic stimuli

1. Hypertrophic alpha-adrenoceptor agonist PE (10 µM) for 48 h. Use serum-free basal medium for dilution. Prepare fresh PE solution from powder before each experiment. Alternatively, treat cells with angiotensin II (100 nM) or endothelin-1 (1, 10, and 100 nM) for 48 h or 24 h, respectively.
2. Cultures of hPSC-CM can be exposed to cyclic equiaxial mechanical stretch. Use 0.5 Hz as the frequency of cyclic stretch with pulsation of 10–25% elongation of cells for 24 h. Cells are stretched by applying a cyclic vacuum suction under Bioflex plates with computer-controlled equipment

(FX-2000; Flexcell International). Use control cultures on the same plate without stretch.

3.3 Screening molecules for effects on cardiac hypertrophy

In order to determine the effect of protein kinase inhibition on growth in cell size of hPSC-CM, use selective small molecule inhibitors, e.g. p38 inhibitor SB202190 (1 μM, Sigma), PKG inhibitor KT5823 (1 μM), HDAC II inhibitor trichostatin A (0.25 μM), ERK inhibitor PD98059 (10 μM), JNK inhibitor SP600125 (1 μM), GSK3β inhibitor 1-azakenpaullone (10 μM), CaMK II inhibitor KN93 (10 μM), calcineurin inhibitor cyclosporine A (0.2 μM), mTOR inhibitor rapamycin (10 ng/ml), and calcineurin/FKBP inhibitor FK506 (0.1 μM) in the presence or absence of PE for 48 hours. Drug discovery methodologies in cardiac hypertrophy may typically start with a phenotype-based high-throughput screen for small-molecule inhibitors (McKinsey and Kass 2007). Approaches to validate cardiomyocyte hypertrophy responses include gene transduction into isolated cardiomyocytes, use of transgenic and knockout animals, and pharmacological studies, including human stem cell models.

3.4. Antibodies and vital dyes

1. Primary antibodies for immunocytochemistry: anti-Ki67 (proliferation marker, 1:100), anti-ANF (hypertrophy signalling, 1:300, Santa Cruz), anti-troponin T (sarcomere protein, 1:200, Abcam), anti-alpha-actinin (sarcomere protein, 1:500, Sigma-Aldrich) and anti-NFAT (transcription factor, 1:100, ab93628, Abcam) primary antibodies (Figure 2).
2. Detection of primary antibodies: Alexa 488-, Alexa 647- and Alexa 546-conjugated secondary antibodies (all 1:400, ThermoFisher Scientific). Dilute probes in RPMI medium supplemented with B27.

3.5. Gene expression and proteome profiling

To assess gene transcriptional changes, TaqMan chemistry based real-time PCR assays and microfluidic PCR cards are used.

3.6. Instrumentation for 3D high-content image acquisition and analysis

1. 3D high-content screening requires a plate reader equipped with high resolution microscope (typically confocal) for optical sectioning. At image acquisition, we use a spinning disk confocal Opera LX plate reader (PerkinElmer) with triple bandpass filters for 488/561/640 nm and UV (365 nm) wavelengths. Various objectives can be used in the Opera setup: 4× air NA=0.16, 40× air NA=0.6, 60× water NA=1.2. We recommend using either of these two types of multiwell plates: BD Optilux (BD Biosciences)

96-well plate use the 40× air lens, and skirtless CellCarrier (PerkinElmer) clear bottom TC treated 384 well plate use the 60× water lens (see note 5.1).

2. Hardware specifications of the high-content-analysis computer. Volume quantification in a high-content environment is resource intensive and computationally demanding. The speed of the analysis can be maximized by loading and processing as much image data into the memory as the system allows. HCA system server motherboards are designed to accommodate a large amount of memory and suitable servers are commercially available. Use a Tyan FT48-B8812 barebone computer for high-content analysis of the images and quantify cell volume, sarcomere reorganisation and ANF redistribution. Our Tyan FT48-B8812 is equipped with 4 pieces of twelve-core AMD Opteron 6174 CPUs and 256 GB memory. In total 48 threads could run in parallel and the overall computational speed can be further improved with the use of a 1 terabyte NAND flash memory as solid state drive integrated on a PCI express card (Supertalent Raiddrive II). As a very fast hard drive it supported 2.4GB/sec read speed through a PCIe (Gen.2) x8 interface.

4. Methods

4.1. Cardiomyocyte differentiation

Differentiation protocols for production of cardiomyocytes from hPSC, including embryonic and induced pluripotent stem cells, are now efficient, relying on sequential exposure to small molecule modulators that mimic early cardiac development (Burridge et al. 2015). One of the most efficient protocols is:

day 0. Take a Matrigel-coated 6-well plate and culture hESCs in mTESR1 (2 ml/ well). Change media to RPMI-B27 without insulin (2 ml) when hPSC culture (maintained in mTESR1) is between 75-90% confluency (d3-4 after thaw or split). Add selective GSK3β inhibitor CHIR99021 at 6μM or 8μM to each well (using 10 mM stock). Optimal level and duration of CHIR99021 can be tested with 6μM or 8μM for both 1 day and 2 days incubation. CHIR99021 is stable at 4 ^{o}C for a minimum of 2-4 weeks.
day 1. Exchange media to RPMI-B27 without insulin, if CHIR99021 is used for one day.
day 2. Exchange media to RPMI-B27 without insulin if CHIR99021 is used for two days.

day 3. Add 2ml RPMI-B27 without insulin and with Wnt pathway inhibitor such as C59 (2.5μM). Change media every two days when feeding cells with RPMI-B27 without insulin.
days 11-13. For metabolic selection, replace media with glucose-free RPMI basal medium (Life Technologies: 11879-020) supplemented with B27. Exposing the cells for 2-4 days with this media selects against proliferating non-cardiomyocytes (see notes 5.2 and 5.3).

4.2 Gene expression assays

Experiments by the authors and others suggest mRNA levels of natriuretic peptides do not usually predict their protein levels. Therefore, a combination of mRNA levels of ANF versus an imaging-based assessment of ANF is expected to work better than either approach alone to clarify disease mechanisms.

1. Lyse undifferentiated and differentiated hESC and hiPSC cultures in TriReagent buffer (Sigma Aldrich) for total RNA extraction. As controls, obtain total RNA from foetal heart (Clontech) and foetal fibroblast (MRC5 lung foetal fibroblast line, ATCC). Purify RNA using RNeasy columns (Qiagen), quantify, and check for quality.
2. Use the High Capacity cDNA Reverse Transcription Kit (ThermoFisher Scientific) to generate double-stranded cDNA.

For quantifying mRNA levels of ANF in undifferentiated hESC and hiPSC cultures, foetal lung fibroblast (MRC5), adult isolated ventricular myocytes, hESC-CM and hiPSC-CM, real-time PCR analyses are performed with TaqMan Gene Expression Assays (ThermoFisher Scientific). Use GAPDH Endogenous Control (FAM/MGB TaqMan gene expression probe, ThermoFisher Scientific) as a housekeeping control. By calculating the gene expression stability measure M, which is the mean pair-wise variation for a gene from all other tested genes, GAPDH is considered as stable reference gene. GAPDH and ACTB show similar stability, as measured with coefficient of variation and standard deviation.

4.3 Phospho-kinase assay. Downstream signalling pathways can be assessed by using proteome screening for kinase phosphorylation. In many cases, despite the significant functional responses in hypertrophy-related parameters, evidence of active signalling was seen in hPSC-CM. Seed hPSC-CM in 6-well plates and treat with pro-hypertrophic agents such as PE (10 μM) for 48 h. Collect cells by centrifugation and wash once with

phosphate buffered saline (PBS). Resuspend cell pellets in lysis buffer and incubate for 20 min at 4 °C. Determine protein concentration using the Pierce protein assay reagent. Perform screening for different phospho-kinases in cell lysates with a Human Phospho-Kinase Antibody Array (R&D Systems).

4.4. High content imaging of hPSC-CM

4.4.1 Live staining and immunocytochemistry.

1. To perform live staining, use high purity cardiomyocyte populations. Add drugs 3 to 5 days after cell plating or recovery from frozen stocks. After drug treatment, incubate cells with Cell Tracker Red (ThermoFisher Scientific) for 45 minutes at 37 ºC with 5% CO_2. Place cells in 100µl fresh media (RPMI-B27) in 96-well or 384-well plate. Keep labelled cultures at 37 °C / 5% CO_2 and scan using automated microscope.
2. To characterize detailed hypertrophic properties of hPSC-CM, use combinations of immunocytochemistry markers. Fix cells with 4% paraformaldehyde, permeabilise with 0.2% Triton X-100, block with 4% foetal bovine serum in PBS for 1 hour and label with anti-ANF (Santa Cruz, sc20518, 1:300), and anti-troponin I (Abcam, ab47003, 1:200) primary antibodies. Use Alexa 488-, and Alexa 546- conjugated secondary antibodies (all 1:400, ThermoFisher Scientific, in 3% bovine serum albumin in PBS as a carrier solution). Use Hoechst (0.5 µg/ml; Sigma-Aldrich) to visualise DNA.

4.4.2 Cell proliferation in fixed cardiomyocytes cultures. Although proliferation rates in hPSC-CM are initially far higher than in adult cardiomyocytes, these drop around one month after differentiation. Cell morphology is initially less organised, but can become more ordered with time or external physical cues. As our earlier data show that PE can increase cell size independently from cell cycle, use of a cell proliferation assay may serve as an internal control.
1. Fix cells after drug treatment and stain with anti-troponin I or anti-alpha-actinin with Alexa 488; anti-Ki67 with Alexa 568; and Hoechst.
2. Quantitate DNA content and visualise DNA intensity as a histogram. Quantitate percentage of 2N and 4N DNA content subpopulations. Quantitate the ratio of Ki67-positive (or phospho-Histone H3-positive) nuclei in the culture to assess proliferating fraction of the population.

4.4.3 2D image acquisition.

1. For 2D acquisition, scan plates on high-content analysis instrument platforms using modified bioapplication protocols for morphology assessment or compartmental analysis. Using an automated highly sensitive fluorescence imaging microscope with 10× objective and suitable filter sets, the stained cells can be identified with Hoechst, antibody against cardiac specific sarcomere protein (such as troponin I or alpha-actinin) 488 and ANF.
2. When the cardiomyocyte undergoes hypertrophy, we expect an orchestrated induction in cell size, sarcomere alignment and cytoplasmic ANF redistribution (Figure 3 shows example images of positive and negative controls). As assay readouts, use cell size; sarcomere content; alignment/abnormalities and length; ANF intensity and distribution; and nuclear translocation of transcription factors such as NFAT (Hinson et al. 2015).

Higher magnification Opera images can be acquired either using a 40× air or a 60× water immersion objective. However, with the Opera system one encounters plate restrictions when working with a water immersion objective. The water holder collar on the objective will not fit under the skirt of a 96- or 384-well plate. Therefore, the Opera can only image skirtless plates with a water immersion objective, and currently those are only available in 384-well format. The Opera Phenix system (PerkinElmer) allows the use of water immersion objectives with 96-well plates with skirt on a restricted plate area, omitting the edge wells. The skirtless CellCarrier-96 Ultra plate (PerkinElmer) will allow the imaging all 96-wells with a water immersion objective. It is at pre-release test phase at the time of writing the manuscript.

4.4.4 3D image acquisition

Here we present an image acquisition protocol for both a 40× air objective and a 60× water immersion objective, combining the latter with the PreScanReScan approach.

40× air objective (96-well plate, BD Optilux, BD Biosciences)

1. Use Opera LX plate reader for image acquisition. Apply 40× air NA=0.6 objective to image the cells seeded into BD Optilux (BD Biosciences) 96 well plates. Apply 30 ms exposure time at the Hoechst channel 1 (365 nm) for nuclear imaging; 400 ms with 3330 μW laser power at the MHC α/β-Alexa 488 in channel 2 (488 nm); and 400 ms with 1600 μW laser power at the ANF-Alexa546 in channel 3 (561 nm). Camera pixels can be binned by 2, resulting in a nominal pixel size of 0.32 μm x 0.32 μm with 1.0 μm axial resolution of the imaged 6 optical slices. Image 25 fields of view (FoV) in the central position of each well.

60× water immersion objective with PreScanReScan (384-well plate, CellCarrier, PerkinElmer)

Use the PreScanReScan system (version 0.91 (10/02/2012) by Achim Kirsch, PerkinElmer Cellular Technologies Germany GmbH), a set of Acapella scripts to (i) prescan with a low magnification objective to identify the location of cardiomyocytes in each well and (ii) rescan those locations with high magnification objective and acquire an image stack. The PreScanReScan can only be run from the Acapella Player environment, and version 0.91 requires Opera software version 2.0 or later.

1. Start the prescan component of the system with imaging the cells, seeded on a CellCarrier (PerkinElmer) clear bottom TC treated 384-well plate. Use a 4× air NA=0.16 objective for the prescanning, applying 500 ms exposure time at the Hoechst channel 1 (365 nm) for nuclear imaging; 800 ms with 3330 μW laser power at the MHC α/β-Alexa 488 in channel 2 (488 nm); and 800 ms with 1600 μW laser power at the ANF-Alexa546 in channel 3 (561 nm)). The camera pixels are not binned resulting in a nominal pixel size of 1.6 μm x 1.6 μm for the imaged optical slice. This 1 FoV (2219 μm x 1677 μm) covers the central region of the well.
2. Execute the first Acapella script component of the PreScanReScan system, "PreScanReScan_Create_Sublayouts_Objects_framelimit.script", on the prescanned images, in order to analyse, identify and record the in-well position of the cells. Each detected cell is supposed to fit in the 60x rescan FoV. The maximum number of cells can be specified in the "framelimit" option. In this example, record the Sublayout of the first 10 cells.
3. Several input parameters are requested by the script file. Besides trivial ones such as "Path to the OperaDB", "Path to the Images:Illustrations" and "Magnification of next lens"(= 60), other parameters need some additional effort in optimisation. The "Offset in X direction, [μm]" and "Offset in Y direction, [μm]" parameters are two experimentally specified constants that represent the offset between the centres of the low and high resolution images. Signs indicate directionality, with negative values virtually shifting the 60x FoV left and up in X and Y directions respectively. Use X offset = -230 μm and Y offset = -150 μm values, which are surprisingly large when we compare the 146 μm x 110 μm size of a whole 60x FoV.

The Image Analysis section specifies the image processing parameters that result in the identification of rescan FoVs. The PreScanReScan algorithm is designed to identify rescan FoVs based on the location of nuclei. However, in this study, cells express strong signal at 488 nm; therefore channel 2, the MHC α/β-Alexa 488 channel, is used ("Channel for Cell Detec-

tion"), providing an intensity filter at the same time. Use the value 100 for size filter ("Minimum Nuclei Size for Rescan"). Instead of nuclei, tune the "Nuclei Detection" section for whole cell detection, using the following parameters:

- Nuclei Detection Algorithm = "A", which is a proprietary segmentation algorithm.
- Threshold Adjustment = 1.5, which ranges from 0 to 3, and fine tunes the segmentation by shrinking (low values) or expanding (high values) the mask.
- Minimum Nuclei Distance = 7, which splits artificially merged nuclei by specifying a minimal distance between centres of nuclei.
- Nuclear Splitting Adjustment = 7, which is another parameter to split artificially merged nuclei.
- Individual Threshold Adjustment = 0.4, which ranges from 0 to 1.0, and fine tunes the segmentation of nuclei.
- Minimum Nuclear Area = 100, which is a size filter in terms of pixels. Discard objects smaller than the specified value.
- Discard minimum Nuclear Contrast = 0.35, which ranges from 0 to 1.0, and is an intensity filter for objects with contrast less than the specified value.
- Parameter SCAN = "None", which is intended for optimisation of the parameters above.

4. Acquire images of the 384-well plate with a 60× water NA=1.2 objective. A 100 ms exposure time can be applied at the Hoechst channel 1 (365 nm) for nuclear imaging; 800 ms with 3330 μW laser power at the MHC α/β-Alexa 488 in channel 2 (488 nm); and 800 ms with 1600 μW laser power at the ANF-Alexa546 in channel 3 (561 nm). Camera pixels are not binned, resulting in a nominal pixel size of 0.11 μm x 0.11 μm with 0.5 μm axial resolution of the imaged 12 optical slices.
5. Determine the number and position of image stacks by the PreScan-ReScan Opera scripts (maximum 10 stacks per well). Use the script collection PreScanReScan version 0.91-2012-02-10 with Opera software 2.0 to identify the location of the cells within each well of the 384-well plate prescanned with 4× objective. Segment cells detected in channel 2 and filter by minimum contrast > 0.35, and area > 100 for rescan at 60× magnification (Figure 4).

4.4.4 3D Fluorescence Image Processing

A diagram of the 3D high-content analysis workflow is shown in Figure 5.

Hardware

Use a server-grade Tyan FT48-B8812 barebone computer; the specifications are described at section 3.5.

Software

Perform the image analysis under a 64-bit version of Kubuntu Linux 10.10, ImageJ version 1.45s and Fiji (Schindelin et al. 2012) with Java 1.6.0_20.

Acquire the 3-channel, fluorescence, 12-bit depth images as Opera LX *.flex files, and analyse after conversion into *.tif format by the Acapella FlexToVolocity.script.

Feature extraction

Extract three features of interest from the images using Fiji: (i) cell volume; (ii) texture features related to sarcomere reorganisation; and (iii) ANF distance from the nucleus related to ANF redistribution.

Cell volume measurement

Perform cell volume measurement on MHC α/β-Alexa 488 in channel 2 images. The image resolution does not allow us to separate each individual cell; therefore calculate the average cell volume in each well by the total volume of the stained voxels divided by the number of nuclei. Perform the 3D cell volume measurement by a custom Fiji macro. The workflow starts with manual selection of a suitable threshold (= 273) that provides optimal segmentation results both at the lowest and highest optical slices. The 3D Object Counter plugin (Bolte and Cordelieres 2006) implemented under Fiji can be used for a 26 neighbour connection, size filter and volume measurement of the foreground voxels. The gelatine cover on the well bottom results in an image noise corrected by a size filter that removes objects smaller than 166 μm^3 (1000 voxel at 40×, 27400 voxel at 60× magnification). Record the 3D object map of each image stack for quality control purposes. Record the volume of each 26 neighbour-connected 3D object, together with its well and field of view identifiers. Measure the nuclear number and position by custom ImageJ macros, which create a maximum intensity projection of the optical slices, and apply a local maxima finder algorithm with noise tolerance = 500. Perform the texture measurement by a custom ImageJ macro using the plugin GLCM Texture Too. Determine cellular foreground area by applying a 10 pixel radius median filter on the maximum intensity projection of a channel 2 image converted to 8-bit, and

segment with threshold = 6. Measure texture features on the maximum intensity projection pixel intensities of channel 2 under the binary mask.

3D localisation
Measure the ANF position in the cell with a custom ImageJ macro that applies a maximum intensity projection of the channel 3 optical slices, and the macro records of the coordinates of local pixel maxima with noise tolerance = 200.

4.4.5 Statistical Data Analysis for Widefield and Confocal High Content Screens

The volumetric, texture and distributional results of the image analysis are stored in ASCII tables and can be evaluated statistically with R, the well-established, open source statistical software (R Development Core Team 2016) (http://r-project.org). Use R scripts to calculate single values per well for (i) average cell volume, (ii) texture descriptors, and (iii) average ANF distance to the centre of the nucleus. Calculate the average cell volume as a ratio of the total volume of MHC α/β-Alexa and total number of nuclei in each well. Calculate the mean value of the texture features in each field of view in a separate R script. Quantify the ANF redistribution by the mean Euclidean ANF distance from the closest nucleus (Figure 3).

Use the cellHTS2 package (Boutros et al. 2006) in custom R scripts for statistical analysis. Normalise the results by a robust Z score method using the median and the median absolute deviation (MAD) of the sample wells. Following normalisation, calculate the Z score of each well, based on the sample workflow described in “End-to-end analysis of cell based screens: from raw intensity readings to the annotated hit list” (last retrieved on 15/02/2016 from the website https://www.bioconductor.org/packages/3.3/bioc/vignettes/cellHTS2/inst/doc/cellhts2Complete.pdf).

Regarding replicates, consider biological replicates to be a batch of differentiated cardiomyocytes taken though a complete experiment (a run of high content microscopy or real time PCR data) (see note 5.4). Technical replicates refer to numbers of repeats within a run for real time PCR and number of wells for high content microscopy. Data from each well for the 2D high content microscopy will be taken from up to 2000 cells, but this is only represented as one value for each well.

Conclusion

Providing multiple endpoints is a great advantage of high content imaging-based assays. The assays can therefore readily predict molecular targets as well as off-target effects of test compounds, such as cytotoxicity or changes in cardiovascular cell morphology. Toxicology and early stages of drug discovery benefit enormously from the advanced 3D high-content screening systems that were, until recently, primarily employed in low-throughput research.

5. Notes

5.1. Only a skirtless plate can operate with a water immersion lens, because a plate skirt hinders the free access of edge wells of an objective with water collar.

5.2. Regarding differentiation of cardiomyocytes, at day 1 check cell morphology at 20x magnification to predict if differentiated cells are going to beat. Cells at the border of the wells should be square and tightly joined and look grey where cells in the middle of cultures are triangular and edged and have gap in between and look “shiny”. On days 9-11 one can see cardiomyocyte contraction (start depends on hPSC-CM line). Once cells start beating, feed them with RPMI-B27 containing insulin.

5.3. Regarding metabolic selection, cardiomyocytes rely on oxidative phosphorylation, while the non-cardiomyocytes tend to rely on glycolysis. Using metabolic selection, cells relying on glycolysis die and only cardiomyocytes survive.

5.4. This is the typical understanding of biological replicates from a cell lines such as HEK or CHO. (For in-house experiments this would usually include the differentiation of a new batch of hESC or hiPSC-derived cardiomyocytes, but this may not be possible from commercial lines where one is reliant on available batch numbers). In many of the experiments here we also have a number of different lines, which can also be considered biological replicates.

6. References

Abramoff, MD, Magalhaes, PJ, and Ram, SJ (2016). Image Processing with ImageJ. Biophotonics International 7(4), 36-43

Aggarwal P, Turner A, Matter A, Kattman SJ, Stoddard A, Lorier R, Swanson BJ, Arnett DK, Broeckel U (2014). RNA expression profiling of human iPSC-derived cardiomyocytes in a cardiac hypertrophy model. PLoS One 9(9):e108051

Ansari N, Muller S, Stelzer EH, Pampaloni F (2013). Quantitative 3D cell-based assay performed with cellular spheroids and fluorescence microscopy. Methods Cell Biol 113:295-309

Bolte S and Cordelieres FP (2006). A guided tour into subcellular colocalization analysis in light microscopy. J Microsc 224(3):213-32

Bosman A, Letourneau A, Sartiani L, Del LM, Ronzoni F, Kuziakiv R, Tohonen V, Zucchelli M, Santoni F, Guipponi M, Dumevska B, Hovatta O, Antonarakis SE, Jaconi ME (2015). Perturbations of heart development and function in cardiomyocytes from human embryonic stem cells with trisomy 21. Stem Cells 33(5):1434-46

Boutros M, Bras LP, Huber W (2006). Analysis of cell-based RNAi screens. Genome Biol 7(7):R66

Bruckner R, Mugge A, Scholz H (1985). Existence and functional role of alpha 1-adrenoceptors in the mammalian heart. J Mol Cell Cardiol 17(7):639-45

Bupha-Intr T, Haizlip KM, Janssen PM (2012). Role of endothelin in the induction of cardiac hypertrophy in vitro. PLoS One 7(8):e43179

Burridge PW, Holmstrom A, Wu JC (2015). Chemically defined culture and cardiomyocyte differentiation of human pluripotent stem cells. Curr Protoc Hum Genet 87:21

Carlson C, Koonce C, Aoyama N, Einhorn S, Fiene S, Thompson A, Swanson B, Anson B, Kattman S (2013). Phenotypic screening with human iPS cell-derived cardiomyocytes: HTS-compatible assays for interrogating cardiac hypertrophy. J Biomol Screen;18(10):1203-11

Carvajal-Vergara X, Sevilla A, D'Souza SL, Ang YS, Schaniel C, Lee DF, Yang L, Kaplan AD, Adler ED, Rozov R, Ge Y, Cohen N, Edelmann LJ, Chang B, Waghray A, Su J, Pardo S, Lichtenbelt KD, Tartaglia M, Gelb BD, Lemischka IR (2010). Patient-specific induced pluripotent stem-cell-derived models of LEOPARD syndrome. Nature 465(7299):808-12

Concas V, Laurent S, Brisac AM, Perret C, Safar M (1989). Endothelin has potent direct inotropic and chronotropic effects in cultured heart cells. J Hypertens Suppl 7(6):S96-S97

Copeland J and Shamu CE (2016). Informatics considerations. An introduction to high content screening, Wiley. 81-102

Dambrot C, Braam SR, Tertoolen LG, Birket M, Atsma DE, Mummery CL (2014). Serum supplemented culture medium masks hypertrophic phenotypes in human pluripotent stem cell derived cardiomyocytes. J Cell Mol Med 18(8):1509-18

Debnath J and Brugge JS (2005). Modelling glandular epithelial cancers in three-dimensional cultures. Nat Rev Cancer 5(9):675-88

Drawnel FM, Archer CR, Roderick HL (2013). The role of the paracrine/autocrine mediator endothelin-1 in regulation of cardiac contractility and growth. Br J Pharmacol 168(2):296-317

Drawnel FM, Boccardo S, Prummer M, Delobel F, Graff A, Weber M, Gerard R, Badi L, Kam-Thong T, Bu L, Jiang X, Hoflack JC, Kiialainen A, Jeworutzki E, Aoyama N, Carlson C, Burcin M, Gromo G, Boehringer M, Stahlberg H, Hall BJ, Magnone MC, Kolaja K, Chien KR, Bailly J, Iacone R (2014). Disease modeling and phenotypic drug screening for diabetic cardiomyopathy using human induced pluripotent stem cells. Cell Rep 9(3):810-21

Foldes G, Matsa E, Kriston-Vizi J, Leja T, Amisten S, Kolker L, Kodagoda T, Dolatshad NF, Mioulane M, Vauchez K, Aranyi T, Ketteler R, Schneider MD, Denning C, Harding SE (2014). Aberrant alpha-adrenergic hypertrophic response in cardiomyocytes from human induced pluripotent cells. Stem Cell Reports 3(5):905-14

Foldes G, Mioulane M, Wright JS, Liu AQ, Novak P, Merkely B, Gorelik J, Schneider MD, Ali NN, Harding SE (2011). Modulation of human embryonic stem cell-derived cardiomyocyte growth: a testbed for studying human cardiac hypertrophy? J Mol Cell Cardiol 50(2):367-76

Ghosh RN, Lapets O, Haskins JR (2007). Characteristics and value of directed algorithms in high content screening. Methods Mol Biol 356:63-81

Hansen A, Eder A, Bonstrup M, Flato M, Mewe M, Schaaf S, Aksehirlioglu B, Schwoerer AP, Uebeler J, Eschenhagen T (2010). Development of a drug screening platform based on engineered heart tissue. Circ Res 107(1):35-44

Hinson JT, Chopra A, Nafissi N, Polacheck WJ, Benson CC, Swist S, Gorham J, Yang L, Schafer S, Sheng CC, Haghighi A, Homsy J, Hubner N, Church G, Cook SA, Linke WA, Chen CS, Seidman JG, Seidman CE (2015). HEART DISEASE. Titin mutations in iPS cells define sarcomere insufficiency as a cause of dilated cardiomyopathy. Science 349(6251):982-6

Ketteler R and Kriston-Vizi J (2016). High-Content Screening in Cell Biology. In: R Bradshaw and P Stahl, eds Encyclopedia of Cell Biology, 4 edn. Academic Press, Waltham, MA. pp. 234-44

Kijlstra JD, Hu D, Mittal N, Kausel E, van der Meer P, Garakani A, Domian IJ (2015). Integrated Analysis of Contractile Kinetics, Force Generation, and Electrical Activity in Single Human Stem Cell-Derived Cardiomyocytes. Stem Cell Reports 5(6):1226-38

Kunz-Schughart LA, Freyer JP, Hofstaedter F, Ebner R (2004). The use of 3-D cultures for high-throughput screening: the multicellular spheroid model. J Biomol Screen 9(4):273-85

Lan F, Lee AS, Liang P, Sanchez-Freire V, Nguyen PK, Wang L, Han L, Yen M, Wang Y, Sun N, Abilez OJ, Hu S, Ebert AD, Navarrete EG, Simmons CS, Wheeler M, Pruitt B, Lewis R, Yamaguchi Y, Ashley EA, Bers DM, Robbins RC, Longaker MT, Wu JC (2013). Abnormal calcium handling properties underlie familial hypertrophic cardiomyopathy pathology in patient-specific induced pluripotent stem cells. Cell Stem Cell 12(1):101-13

Lin B, Li Y, Han L, Kaplan AD, Ao Y, Kalra S, Bett GC, Rasmusson RL, Denning C, Yang L (2015). Modeling and studying mechanism of dilated cardiomyopathy using induced pluripotent stem cells derived from Duchenne Muscular Dystrophy (DMD) patients. Dis Model Mech 8(5):457-66

McKinsey TA and Kass DA (2007). Small-molecule therapies for cardiac hypertrophy: moving beneath the cell surface. Nat Rev Drug Discov 6(8):617-35

Pampaloni F, Reynaud EG, Stelzer EH (2007). The third dimension bridges the gap between cell culture and live tissue. Nat Rev Mol Cell Biol 8(10):839-45

R Core Development Team (2016). A Language and Environment for Statistical Computing. R Foundation for Statistical Computing.Vienna, Austria.

Ren R, Oakley RH, Cruz-Topete D, Cidlowski JA (2012). Dual role for glucocorticoids in cardiomyocyte hypertrophy and apoptosis. Endocrinology 153(11):5346-60

Rokosh DG, Stewart AF, Chang KC, Bailey BA, Karliner JS, Camacho SA, Long CS, Simpson PC (1996). Alpha1-adrenergic receptor subtype mRNAs are differentially regulated by alpha1-adrenergic and other hypertrophic stimuli in cardiac myocytes in culture and in vivo. Repression of alpha1B and alpha1D but induction of alpha1C. J Biol Chem 271(10):5839-43

Schaaf S, Shibamiya A, Mewe M, Eder A, Stohr A, Hirt MN, Rau T, Zimmermann WH, Conradi L, Eschenhagen T, Hansen A (2011). Human engineered heart tissue as a versatile tool in basic research and preclinical toxicology. PLoS One 6(10):e26397

Schindelin J, Arganda-Carreras I, Frise E, Kaynig V, Longair M, Pietzsch T, Preibisch S, Rueden C, Saalfeld S, Schmid B, Tinevez JY, White DJ, Hartenstein V, Eliceiri K, Tomancak P, Cardona A (2012). Fiji: an open-source platform for biological-image analysis. Nat Methods 9(7):676-82

Shamir ER and Ewald AJ (2014). Three-dimensional organotypic culture: experimental models of mammalian biology and disease. Nat Rev Mol Cell Biol 15(10):647-64

Tanaka A, Yuasa S, Mearini G, Egashira T, Seki T, Kodaira M, Kusumoto D, Kuroda Y, Okata S, Suzuki T, Inohara T, Arimura T, Makino S, Kimura K, Kimura A, Furukawa T, Carrier L, Node K, Fukuda K (2014). Endothelin-1 induces myofibrillar disarray and contractile vector variability in hypertrophic cardiomyopathy-induced pluripotent stem cell-derived cardiomyocytes. J Am Heart Assoc 3(6):e001263

Vinci M, Gowan S, Boxall F, Patterson L, Zimmermann M, Court W, Lomas C, Mendiola M, Hardisson D, Eccles SA (2012). Advances in establishment and analysis of three-dimensional tumor spheroid-based functional assays for target validation and drug evaluation. BMC Biol 10:29

Wang G, McCain ML, Yang L, He A, Pasqualini FS, Agarwal A, Yuan H, Jiang D, Zhang D, Zangi L, Geva J, Roberts AE, Ma Q, Ding J, Chen J, Wang DZ, Li K, Wang J, Wanders RJ, Kulik W, Vaz FM, Laflamme MA, Murry CE, Chien KR, Kelley RI, Church GM, Parker KK, Pu WT (2014). Modeling the mitochondrial cardiomyopathy of Barth syndrome with induced pluripotent stem cell and heart-on-chip technologies. Nat Med 20(6):616-23

Wu H, Lee J, Vincent LG, Wang Q, Gu M, Lan F, Churko JM, Sallam KI, Matsa E, Sharma A, Gold JD, Engler AJ, Xiang YK, Bers DM, Wu JC (2015). Epigenetic Regulation of Phosphodiesterases 2A and 3A Underlies Compromised beta-Adrenergic Signaling in an iPSC Model of Dilated Cardiomyopathy. Cell Stem Cell 17(1):89-100

Zhi D, Irvin MR, Gu CC, Stoddard AJ, Lorier R, Matter A, Rao DC, Srinivasasainagendra V, Tiwari HK, Turner A, Broeckel U, Arnett DK (2012). Whole-exome sequencing and an iPSC-derived cardiomyocyte model provides a powerful platform for gene discovery in left ventricular hypertrophy. Front Genet 3:92

Zhong H and Minneman KP (1999). Alpha1-adrenoceptor subtypes. Eur J Pharmacol 375(1-3):261-76

Figure Captions

Figure 1. Schematic drawing of various approaches in hypertrophy modelling and drug screening (CRISPR-Cas9 models, pharmacological approaches, patient-derived hiPSC trials *in vitro*).

Figure 2. Cultured human pluripotent stem cell-derived cardiomyocytes. **A** Depending on the nature of the stimulus and its intensity (example shows PE treatment in the presence of proliferation / cytokinesis inhibitor agent blebbistatin, 48 hours), hPSC-CM can undergo hypertrophy, activation of cell death pathways or progression into cell division. Cells were stained with Hoechst,; sarcomere protein troponin I or MHC α/β; atrial natriuretic factor ANF; and proliferation marker Ki67. Scale bar 10 μm. **B** Example 3D reconstructions (Volocity) of these cells are also shown.

Figure 3. A Whole plate level visualisation of ANF distribution. Mean ANF-nucleus distances in μm were calculated with an R script and the results are shown as a plate heatmap, generated using the Prada (version 1.42) package from Bioconductor, R (version 3.2.3). Representative images of the wells that show, **B** no change in ANF distribution, and **C** significant changes in ANF distribution.

Figure 4. A Illustration of cardiomyocytes imaged with 4x lens at PreScan step after image analysis. The identified cells were re-imaged with 60x lens in the ReScan step. Yellow rectangles show the contours of the 60x field of views. Scale bar 100 μm. **B** Maximum intensity projection of cardiomyocytes imaged with PerkinElmer Opera, 60x (NA=1.2) water immersion lens. Cells were stained with Hoechst, MHC α/β-Alexa and ANF-Alexa546 on blue, green and red channels and imaged in 365 nm, 488 nm and 561 nm excitation wavelengths respectively. Scale bar 10 μm.

Figure 5. Illustrative diagram of the high-content analysis workflow applied. 3D image stack of confocal slices serves as input and a database of cell volumes is the output. Overlay images play an important role; the workflow quality is checked at every step.

Table Captions

Table 1. Human PSC-derived cardiomyocyte models for inherited disorders with hypertrophic phenotype

Table 2. Phenotypic assays to assess cardiomyocyte hypertrophy.

Glossary

ANF	Atrial natriuretic peptide
BNP	B-type natriuretic peptide
ESC	embryonic stem cell
GSK	glycogen synthase kinase
HCM	hypertrophic cardiomyopathy
hESC	Human embryonic stem cell
hESC-CM	Human embryonic stem cell-derived cardiomyocyte
hiPSC	Human induced pluripotent stem cell
hiPSC-CM	Human induced pluripotent stem cell-derived cardiomyocyte
hPSC	Human pluripotent stem cell
hPSC-CM	Human pluripotent stem cell-derived cardiomyocyte
MAPK	mitogen activated protein kinase
NFAT	nuclear factor of activated T-cells

Acknowledgements

This work was supported by the UK Medical Research Council core funding to the MRC-UCL University Unit (Ref. MC_EX_G0800785) (JKV), the European Union Seventh Framework Programme (FP7/2007-2013, grant no. PIRG08-GA-2010-276811) (JKV), and the Hungarian Scientific Research Fund (OTKA K-105555) (GF).

Condition	Cell Source	Mutation	Cardiac phenotype	Reference
LEOPARD syndrome	hiPSC	Protein tyrosine phosphatase, non-receptor type 11 gene (PTPN11)	Cardiac hypertrophy, electrocardiographic abnormalities, pulmonary valve stenosis	(Carvajal-Vergara et al. 2010)
Hypertrophic cardiomyopathy (HCM)	hiPSC	Missense mutation on exon 18 of the β-myosin heavy chain gene; myosin binding protein C	Non-ischaemic cardiomyopathy, enlargement of the cardiac cells	(Lan et al. 2013; Dambrot et al. 2014)
Dilated cardiomyopathy (DCM)	hiPSC	Point mutation R173W in exon 12 of troponin T2 gene;	Non-ischaemic cardiomyopathy, increased heterogeneous sarcomeric organization	(Sun et al. 2012; Wu et al. 2015; Karakikes et al. 2015)
Barth syndrome	hiPSC	Mutation of gene encoding tafazzin	Cardiomyopathy, cardiolipin abnormalities	(Wang et al. 2014)
Duchenne muscular dystrophy (DMD)	hiPSC	Mutation in DMD gene encoding dystrophin	Muscle degeneration, dysorganised sarcomere	(Lin et al. 2015)
Down's Syndrome	hESC	Trisomy 21	Increased expression of hypertrophic cardiomyopathy genes	(Bosman et al. 2015)

Table 1.

Hypertrophy Assay	Technology	Reference
Mechanical analysis of hypertrophied cells and myocardial tissue constructs	Cardiac microtissue platform; single cell microarray post detectors (mPads); engineered heart tissue; heart-on-chip model; muscular thin film; applied stretch for single cells with Flexercell	(Hinson et al. 2015; Schaaf et al. 2011; Hansen et al. 2010; Wang et al. 2014)
Imaging intracellular changes	Flow cytometry for troponin/BNP-positive cells; spontaneous Ca2+ transient imaging and measurements; translocation of transcription factors; extracellular flux analysis (Seahorse) to detect altered metabolism; traction force microscopy for single cell contractility; Cellular impedance monitoring for cell growth	(Wang et al. 2014; Wu et al. 2015; Tanaka et al. 2014; Kijlstra et al. 2015; Tanaka et al. 2014; Drawnel et al. 2014)
Gene profiling / gene regulatory networks and related pathway analysis	Real time PCR; TaqMan microfluidic cards; Single cell PCR; Small RNA assays; Microarray; RNAseq; miRNASeq; GSEA pre-ranked analysis	(Aggarwal et al. 2014; Hinson et al. 2015; Drawnel et al. 2014)
Production and release of hypertrophic factors	ANF, BNP, ET-1, FABP3, troponin I	(Carlson et al. 2013; Tanaka et al. 2014; Drawnel et al. 2014)
Comparison with engineered or native cells	Isolated human ventricular myocytes; neonatal mouse/rat cells, rat embryonic cardiomyocytes (H9C2); CRISPR/Cas9-isogenic control	(Foldes et al. 2014; Ren et al. 2012; Hinson et al. 2015; Wang et al. 2014)

Table 2.

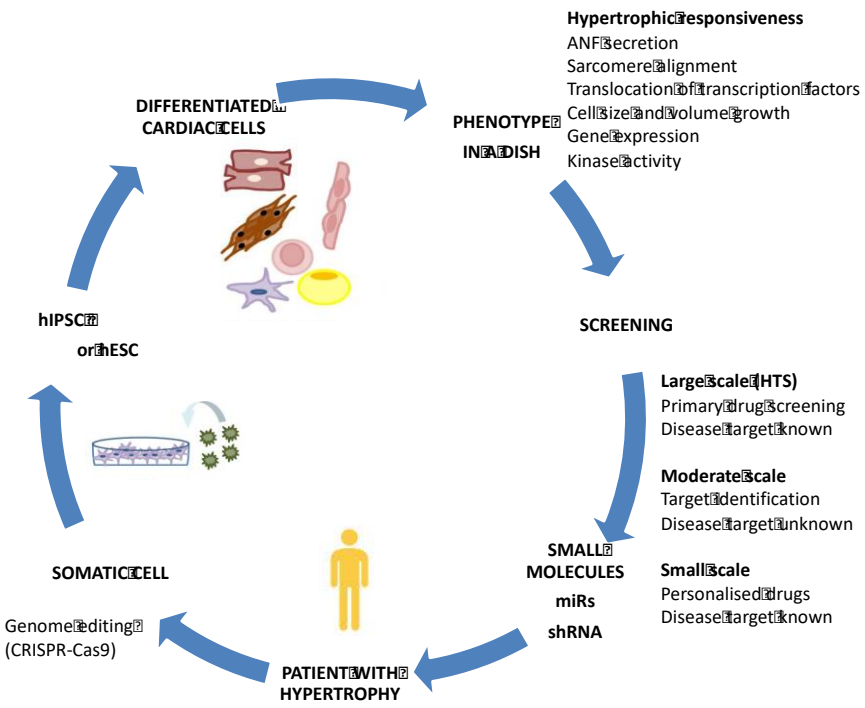
Hypertrophic responsiveness
ANF secretion
Sarcomere alignment
Translocation of transcription factors
Cell size and volume growth
Gene expression
Kinase activity
DIFFERENTIATED CARDIAC CELLS
PHENOTYPE IN A DISH
SCREENING
Large scale (HTS)
Primary drug screening
Disease target known
Moderate scale
Target identification
Disease target unknown
Small scale
Personalised drugs
Disease target known
SMALL MOLECULES
miRs
shRNA
PATIENT WITH HYPERTROPHY
Genome editing (CRISPR-Cas9)
SOMATIC CELL
hIPSC or hESC

Figure 1

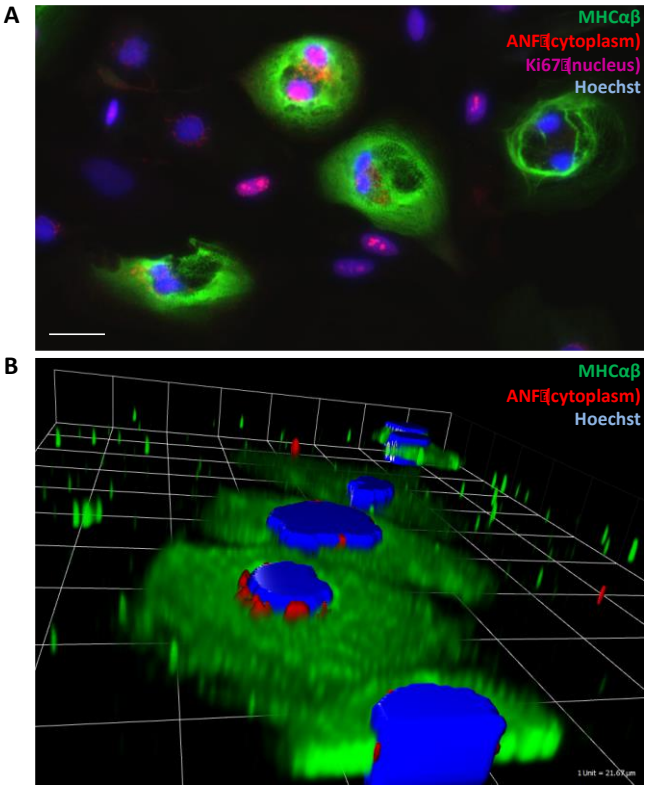
A
MHCαβ
ANF (cytoplasm)
Ki67 (nucleus)
Hoechst
B
MHCαβ
ANF (cytoplasm)
Hoechst

Figure 2

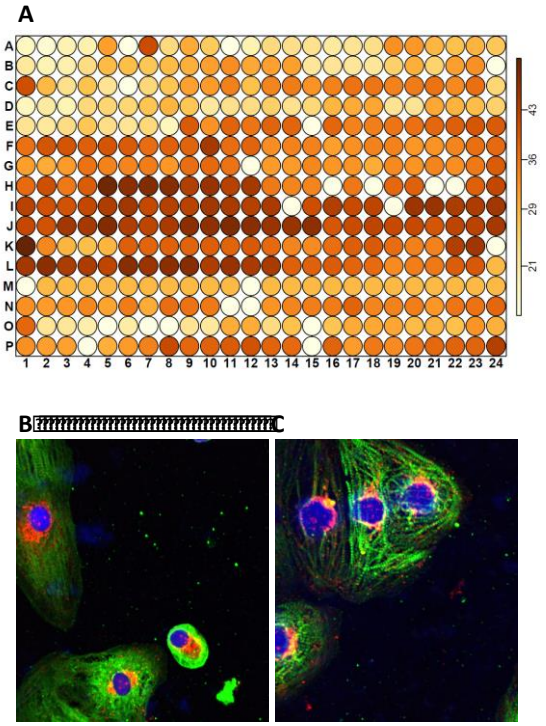
A
A
B
C
D
E
F
G
H
I
J
K
L
M
N
O
P
1 2 3 4 5 6 7 8 9 10 11 12 13 14 15 16 17 18 19 20 21 22 23 24
43
36
29
21
B
C

Figure 3

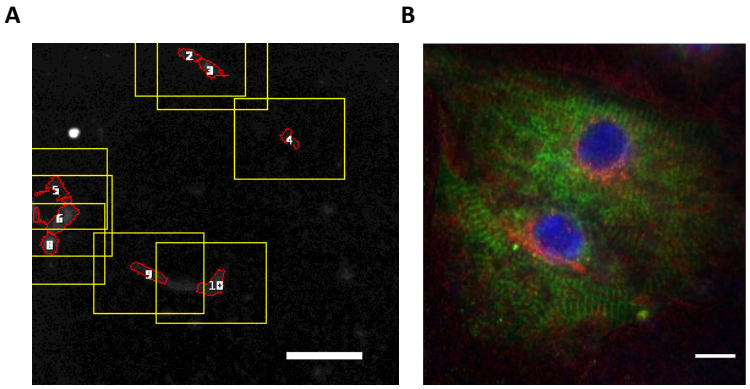

Figure 4

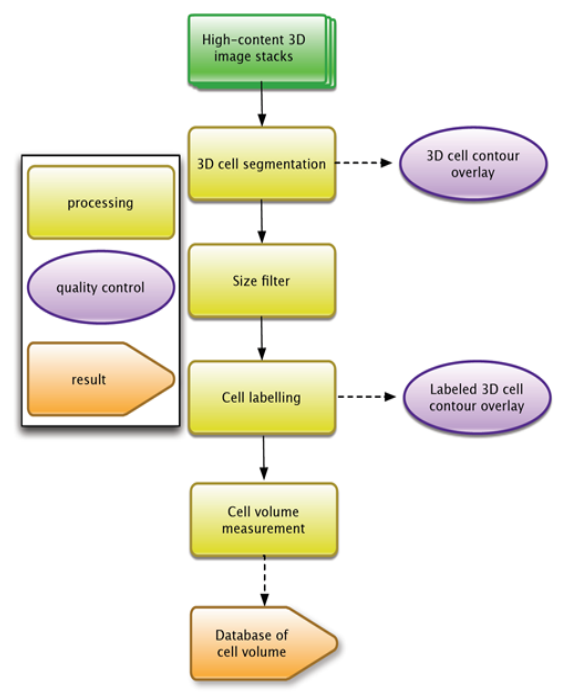
High-content 3D image stacks
3D cell segmentation
3D cell contour overlay
processing
quality control
result
Size filter
Cell labelling
Labeled 3D cell contour overlay
Cell volume measurement
Database of cell volume

Figure 5